J Inorg Organomet Polym (2015) 25:569–575
DOI 10.1007/s10904-014-0118-9

Two New Zn(II)/Cd(II) Coordination Polymers Based on Rigid Squaric Acid: Crystal Structure, Topology and Fluorescent Properties

Ping Tang · Wen-Wen Dong · Wei Xia · Jun Zhao

Received: 14 September 2014 / Accepted: 3 November 2014 / Published online: 11 November 2014

Abstract Presented here are two d^{10} metal–organic coordination polymers (CPs), $[Zn(C_4O_4)_{0.5}(\mu_3\text{-}OH)]_n$ (**1**) and $[Cd(C_4O_4)_{0.5}(OX)_{0.5}(H_2O)]_n$ (**2**) (H_2OX = oxalic acid) constructed from squaric acid ($H_2C_4O_4$) tectons. Single-crystal X-ray diffraction studies indicated that both **1** and **2** show 3D structures. The two 3D CPs are assembled from 1D $\{[Zn(\mu_3\text{-}OH)]_n^+\}$ chains to 3D structure linked through $C_4O_4^{2-}$ ligands for **1** and 2D $\{[(Cd1)_2(C_4O_4)]^{2+}\}$ layers pillared by OX^{2-} ligands for **2**. The structure of compound **1** can be described as a trinodal (3,6,6)-connected net with the point symbol of $\{4^3\}_2\{4^4\cdot6^{10}\cdot8\}\{4^5\cdot6^{10}\}_2$, whereas **2** possess a trinodal (4,5,6)-connected $\{4^2\cdot8^4\}$ $\{4^6\cdot6^6\cdot8^3\}$ $\{4^8\cdot6^2\}_2$ topology. Furthermore, the fluorescent and thermal stabilities properties of these two compounds were investigated.

Keywords Squaric acid · Coordination polymer · Network topology · Fluorescent property

1 Introduction

The design and construction of new functional coordination polymers (CPs) have been one of the pioneer fields in current crystal engineering due to their intriguing topological structures and potential applications in diverse areas (e.g. catalytic, optical, molecular recognition, gas storage/separation, sensors, drug delivery, etc.) [1–5]. At present, large numbers of novel CPs have been designed and synthesized, but the reasonable design and controllable synthesis, however, is difficult to control since the final structure is frequently subject to subtle variation of external parameters, such as solvent [6], temperature [7], pH [8], organic ligands [9], metal cations [10], etc. Among these factors, the organic ligands influence profoundly the specific structures of synthesized products, and to dictate their formation with potential applications [11].

In recent years, the symmetrical, planar and rigid squaric acid has attracted much attention in the preparation of functional polymeric frameworks. It features extensive π-electron delocalization over all the oxygen and carbon atoms, which tends to induce hydrogen-bonding, π–π interactions for the construction of extended frameworks. As well as it has versatile coordination modes, so that it is widely used as a μ_2 to μ_8 bridging ligand bonded with metal ions in various bridging modes (Scheme 1) to create numerous amazing metal–squarate frameworks, including 1-, 2-, and 3-D cube and cage-like frameworks [12–18]. Recently, a few investigative examples of squarate-bridged metal complexes have been reported. For instance, cobalt-base complexes, $Co_3(OH)_2(C_4O_4)_2\cdot3H_2O$ [19] and $Co_3(OH)_2(C_4O_4)_2$ [20] have been observed, which show interesting magnetic properties. Our groups have concentrated on utilizing squaric acid ligands and d^{10} metal ions to constructing novel topological networks [21], as an extension of our work, herein, we report the synthesis, structural characterizations, and fluorescent properties of two new CPs, namely, $[Zn(C_4O_4)_{0.5}(\mu_3\text{-}OH)]_n$ (**1**) and $[Cd(C_4O_4)_{0.5}(OX)_{0.5}(H_2O)]_n$ (**2**).

Electronic supplementary material The online version of this article (doi:10.1007/s10904-014-0118-9) contains supplementary material, which is available to authorized users.

P. Tang · W. Xia
College of Biological and Pharmaceutical Sciences, China Three Gorges University, Yichang 443002, People's Republic of China

W.-W. Dong (✉) · J. Zhao
College of Materials and Chemical Engineering, China Three Gorges University, Yichang 443002, People's Republic of China
e-mail: dongww1@126.com

Scheme 1 Coordination modes of squarate on the construction of coordination polymers

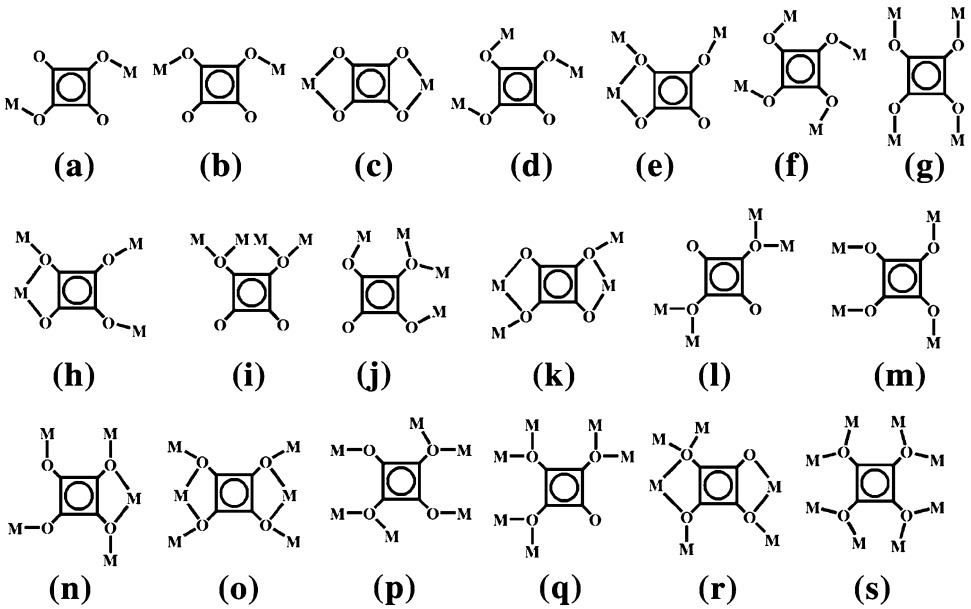

2 Experimental

2.1 Materials and General Methods

All solvents and reagents for syntheses were commercially available and used as received. The infrared spectra (400–4000 cm^{-1}) were recorded as KBr pellets a FTIR Nexus spectrophotometer. Elemental analyses were performed on a Perkin-Elmer 2400 Series II analyzer. X-ray powder diffraction (XRPD) patterns for microcrystalline samples were taken on a Rigaku Ultima IV diffractometer (Cu Kα radiation, $\lambda = 1.5406$ Å), with a scan speed of 8° min^{-1} and a step size of 0.02 deg in 2θ. The calculated XPRD patterns were simulated by using the single-crystal X-ray diffraction data. Thermogravimetric (TGA) curves were recorded on a NETZSCH STA 449C microanalyzer in air atmosphere at a heating rate of 10 °C min^{-1}. Fluorescence spectra were recorded on a Hitachi F-4500 fluorescence spectrophotometer at room temperature.

2.2 Preparation of $[Zn(C_4O_4)_{0.5}(\mu_3\text{-}OH)]_n$ (**1**)

A mixture of $H_2C_4O_4$ (11.4 mg, 0.10 mmol), $Zn(ClO_4)_2{\cdot}6H_2O$ (37.2 mg, 0.10 mmol), and H_2O (6 mL) was stirred at room temperature for 0.5 h. The reaction mixture was transferred to a 25 mL stainless steel reactor with Teflon liner and heated at 140 °C for 72 h. The reaction system was cooled to room temperature and colorless block crystals of **1** were obtained; yield, 67 % (9.23 mg) based on Zn. Anal. Calcd. (%) for C_2HO_3Zn: C, 17.35; O, 34.67; H, 0.73; Found: C, 17.29; O, 34.65; H, 0.78. IR (KBr pellet, cm^{-1}): 3413 (s), 1596 (m), 1560 (m), 1411 (w), 1130 (w), 1095 (s), 848 (w), 799 (w), 714 (w).

2.3 Preparation of $[Cd(C_4O_4)_{0.5}(OX)_{0.5}(H_2O)]_n$ (**2**)

A mixture of $H_2C_4O_4$ (11.4 mg, 0.10 mmol), $Cd(ClO_4)_2{\cdot}6H_2O$ (41.9 mg, 0.10 mmol), H_2OX (12.61 mg, 0.1 mmol), and H_2O (6 mL) was stirred at room temperature for 0.5 h. The solution was transferred to a 25 mL stainless steel reactor with Teflon liner and heated at 140 °C for 72 h. The reaction system was cooled to room temperature and colorless block crystals of **2** were obtained with a yield of 73 % (16.83 mg) based on Cd. Anal. Calcd. (%) for $C_3H_2CdO_5$: C, 15.64; O, 34.71; H, 0.87; Found: C, 15.59; O, 34.77; H, 0.91. IR (KBr pellet, cm^{-1}): 3485 (s), 3256 (m), 1617 (m), 14 92 (s), 1311 (s), 133 (s), 1080 (s), 706 (m), 634 (w).

2.4 X-ray Crystallography

Single-crystal X-ray diffraction analysis of **1** and **2** were carried out on a Rigaku XtaLAB mini diffractometer with graphite monochromated Mo Kα radiation ($\lambda = 0.71073$ Å) by using φ/ω scan technique at 296(2) K. The collected data were reduced using the program CrystalClear [22] and an empirical absorption correction was applied. The structures were solved by direct methods and refined based on F^2 by the full matrix least-squares methods using SHELXTL [23]. The H-atoms were assigned with common isotropic displacement factors and included in the final refinement by use of geometrical restrains. Generally, the positions of the C-bound H-atoms were generated by a riding model on idealized geometries. The crystal qualities of these two compounds were not good enough as indicated by the high R_{int} value [24, 25]. The crystallographic data and selected bond lengths and angles for **1** and **2** are listed in Tables 1 and 2.

Table 1 Crystal data and structure refinement parameters for compounds **1–2**

Compounds	**1**	**2**
Empirical formula	C_2HO_3Zn	$C_3H_2CdO_5$
Formula weight	138.40	230.46
Temperature (K)	296(2)	296(2)
Crystal system, space group	Monoclinic, $P2_1/c$	Monoclinic, $P2_1/n$
a (Å)	3.324(2)	5.995(7)
b (Å)	9.9880(10)	7.454(8)
c (Å)	8.6440(10)	11.401(2)
α (°)	90	90
β (°)	102.090(3)	100.329(14)
γ (°)	90	90
Volume (Å ^{3})	280.62(17)	501.2(8)
Z	4	4
Calculated density (mg m^{-3})	3.276	3.054
Absorption coefficient (mm^{-1})	8.526	4.292
F(000)	268	432
Reflections collected	2,852	5,211
Reflections unique	642 [R(int) = 0.1583]	1,169 [R(int) = 0.1453]
Data/restraints/parameters	4,140/15/382	1,169/3/89
Goodness-of-fit F^2	1.079	1.009
R_1 [$I > 2\sigma(I)$][a]	0.0462	0.0336
wR_2 [$I > 2\sigma(I)$][b]	0.0875	0.0820
R_1 (all data)	0.0475	0.0359
wR_2 (all data)	0.0883	0.0833

[a] $R = \Sigma||F_0| - |F_C||/\Sigma|F_0|$

[b] $wR_2 = [\Sigma[w(F_0^2 - F_C^2)^2]/\Sigma[(F_0^2)^2]]^{1/2}$

3 Results and Discussion

3.1 Crystal Structures Analysis of 1 and 2

Single-crystal X-ray analysis reveals that compounds **1** and **2** both crystallize in the monoclinic system, but in different space group; $P2_1/c$ for **1** and $P2_1/n$ for **2.** The asymmetric unit of **1** contains one independent Zn(II) ion, one OH^- anion, half a $C_4O_4^{2-}$ anion, while the asymmetric unit of **2** contains one Cd(II) ion, half an OX^{2-} anion, half a $C_4O_4^{2-}$ anion and one coordinated water molecule. In **1**, the Zn(II) center shows a distorted octahedral [ZnO_6] sphere composed of six oxygen atoms from three hydroxyls and three $C_4O_4^{2-}$ ligands (Fig. 1). The Zn–O bond lengths are in the range of 2.024(3)–2.543(3) Å, and the bond angles O–Zn–O are vary from 80.14(9)° to 168.28(10)° (Table 2). It should be mentioned that the Zn(1)–O(1)$_{x+1/2,\ -y+3/2,\ z+1/2}$ (2.543(3) Å) bond distance is slightly longer than normal Zn–O bond distances. But it may be considered normal, when compared with the values of 2.550–2.711 Å cited in the literatures [26]. And in general, the long Zn–O distance indicates a relatively weak interaction, which can be considered to be secondary coordination. While for **2**, Cd1 is eight-coordinated by four oxygen atoms from three different $C_4O_4^{2-}$ anions, three oxygen atoms from two different OX^{2-} anions, and one oxygen atom from water molecule (Fig. 2). The disposition of the eight donor atoms can be adequately described as a distorted dodecahedral geometry (Fig. S1). The Cd–O bond distances vary from 2.272(3) to 2.652(6) Å (Table 2). Observed Cd-donor atom bonds are in good agreement with values reported previously for eight-coordinated cadmium complexes [27, 28].

Notably in **1**, the hydroxyl adopts μ_3-bridging coordination mode to link the adjacent Zn(II) ions to form 1D $\{[Zn1(\mu_3\text{-}OH)]_n^+\}$ chain along the a axis (Fig. 3a). Furthermore, through sharing Zn(II) centers, the $C_4O_4^{2-}$ anions in a μ_6-η^1:η^2:η^1:η^2 coordination mode (Scheme 1p) connect these 1D chains to produce a 3D network (Fig. 3b). Besides, in **1,** there exists strong hydrogen-bonding interactions from μ_3-OH group (O3) to O2 from $C_4O_4^{2-}$, (O3···O2 = 2.880 Å, O3–H···O2 = 162°). These weak interactions may make a certain contribution to the additional stability of the whole structure. From a topological point of view, each $C_4O_4^{2-}$ anion can be viewed as a 6-connected node, each Zn(II) as 6-connected node, and each μ_3-OH as 3-connected node, so the whole framework can be defined as a rare trinodal (3,6,6)-connected net with the point symbol of $\{4^3\}_2\{4^4\cdot6^{10}\cdot8\}\{4^5\cdot6^{10}\}_2$ (Fig. 3c).

While in **2**, the $C_4O_4^{2-}$ anions with μ_6-η^2:η^2:η^2:η^2 bridging coordination mode (Scheme 1o) link Cd(II) centers into a 2D $\{[(Cd1)_2(C_4O_4)]^{2+}\}$ layer, which contains two different chains (Fig. 4a). Further examination shows that the two kinds of chains are consisted of four-member rings (purple in Fig. 4a) and ten-member rings (green in Fig. 4a), respectively. And the chains are associated with each other via edge-sharing the Cd–O bonds and result in formation of a 2D layer. Furthermore, the small molecule OX^{2-} with μ_4-η^1:η^2:η^1:η^2 coordination mode serves as pillar to join the neighboring 2D layers to a 3D framework (Fig. 4b). Topological analysis shows that this 3D network can be simplified by considering $C_4O_4^{2-}$ as 6-connected node, OX^{2-} as 4-connected node, and Cd(II) as 5-connected node, so the whole framework can be simplified as a trinodal (4,5,6)-connected network with the point symbol of $\{4^2\cdot8^4\}\ \{4^6\cdot6^6\cdot8^3\}\ \{4^8\cdot6^2\}_2$ (Fig. 5).

It can be clearly seen that the structures of compounds **1** and **2** are different, although they were synthesized by the similar hydrothermal conditions except that different small molecule ligands (OH^- or $C_2O_4^{2-}$) as well as different d^{10} metal ions [Zn(II) or Cd(II)] are employed. As mentioned above, the structure of compound **1** assembled from 1D

Table 2 Selected bond lengths (Å) and angles (°) for **1** and **2**

Compound **1**			
Zn(1)–O(3)#1	2.024(3)	Zn(1)–O(2)#3	2.041(2)
Zn(1)–O(3)#2	2.039(2)	Zn(1)–O(1)	2.161(3)
Zn(1)–O(3)	2.110(3)	Zn(1)–O(1)#4	2.543(3)
O(3)#1–Zn(1)–O(3)#2	109.82(13)	O(3)#2–Zn(1)–O(2)#3	102.94(10)
O(3)#1–Zn(1)–O(2)#3	102.13(9)	O(3)#1–Zn(1)–O(3)	81.70(11)
O(3)#2–Zn(1)–O(3)	85.88(10)	O(2)#3–Zn(1)–O(3)	168.28(10)
O(3)#1–Zn(1)–O(1)	164.19(12)	O(3)#2–Zn(1)–O(1)	84.57(11)
O(2)#3–Zn(1)–O(1)	80.14(9)	O(3)–Zn(1)–O(1)	93.20(8)
Compound **2**			
Cd(1)–O(3)	2.269(3)	Cd(1)–O(5)	2.306(2)
Cd(1)–O(1)	2.335(4)	Cd(1)–O(4)#1	2.296(3)
Cd(1)–O(2)#2	2.450(3)	Cd(1)–O(2)#3	2.520(4)
Cd(1)–O(4)#4	2.599(3)	Cd(1)–O(3)#5	2.652(6)
O(3)–Cd(1)–O(5)	97.92(10)	O(3)–Cd(1)–O(4)#1	160.93(15)
O(3)–Cd(1)–O(1)	91.72(10)	O(4)#1–Cd(1)–O(5)	85.04(10)
O(5)–Cd(1)–O(1)	145.65(10)	O(4)#1–Cd(1)–O(1)	96.38(10)
O(4)#1–Cd(1)–O(2)#2	81.59(9)	O(3)–Cd(1)–O(2)#2	85.40(8)
O(1)–Cd(1)–O(2)#2	68.51(10)	O(5)–Cd(1)–O(2)#2	144.85(10)
O(4)#1–Cd(1)–O(2)#3	81.41(9)	O(3)–Cd(1)–O(2)#3	80.58(9)
O(1)–Cd(1)–O(2)#3	134.33(10)	O(5)–Cd(1)–O(2)#3	79.92(11)
O(3)–Cd(1)–O(4)#4	65.31(12)	O(2)#2–Cd(1)–O(2)#3	66.05(11)
O(5)–Cd(1)–O(4)#4	78.44(11)	O(4)#1–Cd(1)–O(4)#4	133.48(7)
O(2)#2–Cd(1)–O(4)#4	132.76(9)	O(1)–Cd(1)–O(4)#4	75.88(9)
O(2)#3–Cd(1)–O(4)#4	136.11(8)		

Symmetry codes: for **1**, #1 −x − 1, −y + 1, −z; #2 −x, −y + 1, −z; #3 x − 1, −y + 1/2, z − 1/2; #4 x − 1,y, z; for **2**, #1 –x, −y + 2, −z + 1; #2 −x + 1, −y + 2, −z + 1; #3 x − 1, y, z; #4 x + 1/2, −y + 3/2, z + 1/2; #5 –x + 1/2, y + 1/2, −z + 3/2

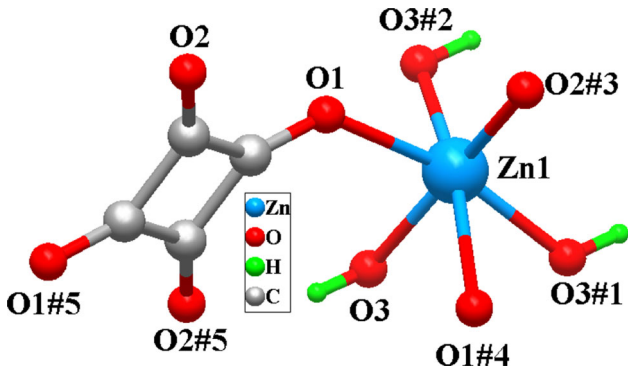

Fig. 1 Coordination environment of the Zn center in compound **1**. Symmetry codes for the generated atoms: #1: −x − 1, −y + 1, −z; #2: −x, −y + 1, −z; #3: x − 1, −y + 1/2, z − 1/2; #4: x − 1, y, z; #5: −x + 1, −y + 1, −z + 1 (Color figure online)

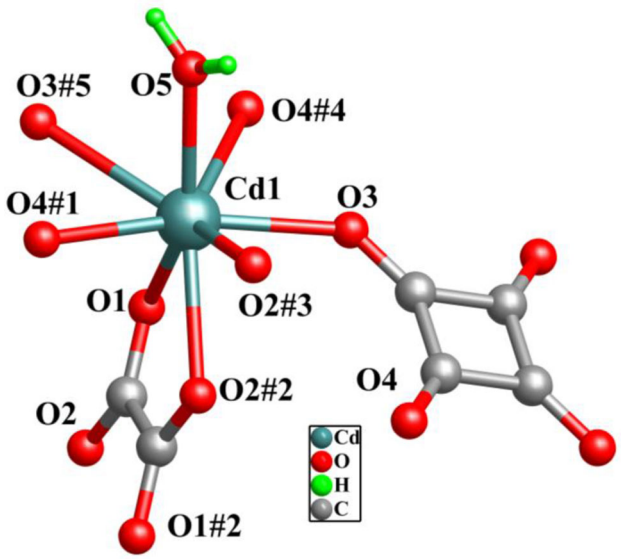

Fig. 2 Coordination environment of the Cd center in compound **2**. Symmetry codes for the generated atoms: #1: −x, −y + 2, −z + 1; #2: −x + 1, −y + 2, −z + 1; #3: x − 1, y, z; #4: x + 1/2, −y + 3/2, z + 1/2; #5: −x + 1/2, y + 1/2, −z + 3/2 (Color figure online)

$\{[Zn(\mu_3\text{-}OH)]_n^+\}$ chains to 3D structure linked through $C_4O_4^{2-}$ ligands for **1,** but 2D $\{[(Cd1)_2(C_4O_4)]^{2+}\}$ layers to 3D network pillared by OX^{2-} ligands for **2.** The structural

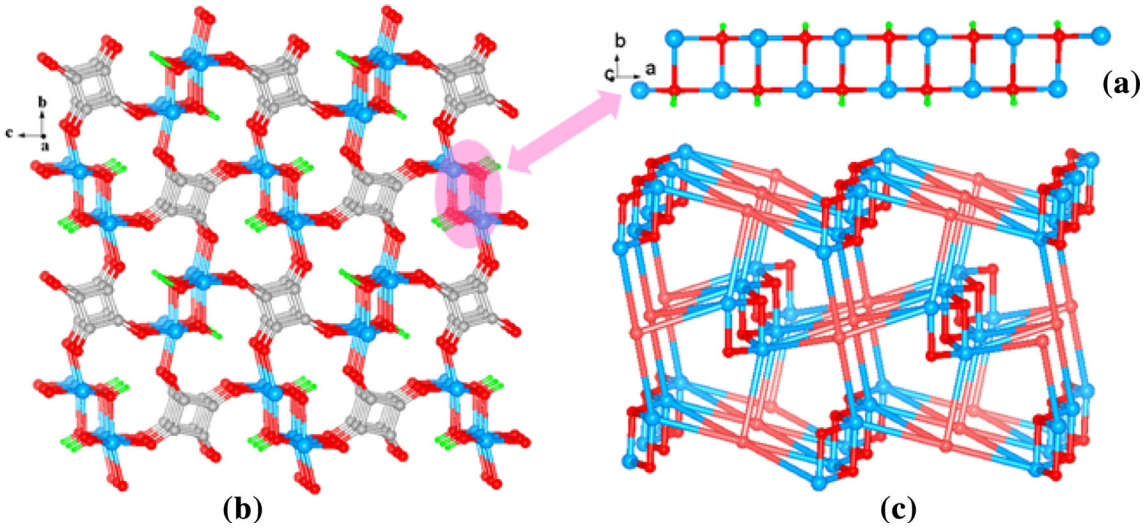

Fig. 3 **a** The 1D $\{[Zn(\mu_3\text{-}OH)]_n^+\}$ chains along *c* axis; **b** view of the 3D structure along the *a* axis. **c** Perspective view of the trinodal (3,6,6)-connected network of **1**. Color codes: *blue* for 6-connected Zn(II), *pink* for 6-connected $C_4O_4^{2-}$ ligand and *red* for 3-connected μ_3-OH (Color figure online)

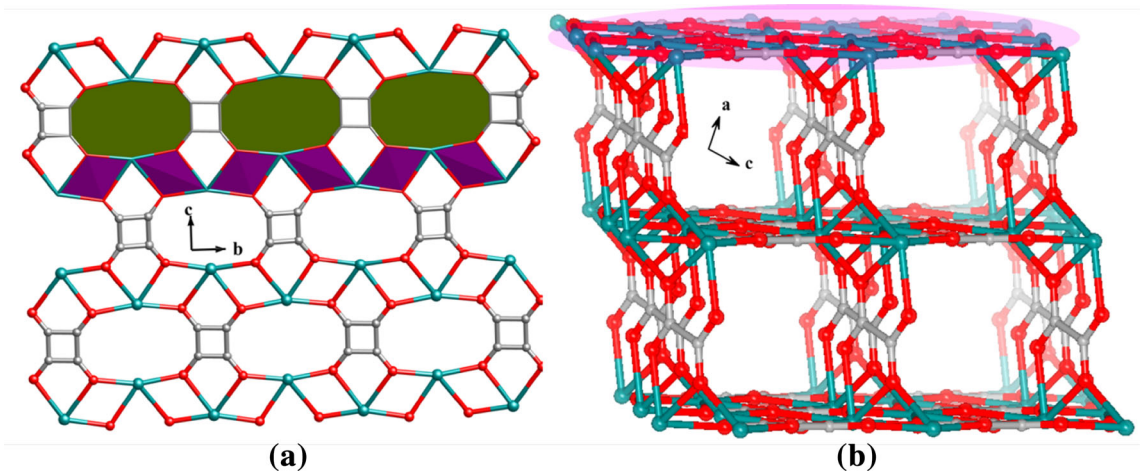

Fig. 4 **a** View of the 2D layer along *a* axis. *Purple* 1D chain consists of four-member rings. *Green* 1D chain consists of ten-member rings; **b** view of the 3D structure of **2**. Hydrogen atoms and water molecules have been omitted for clarity (Color figure online)

difference could mainly arise from the different coordinated modes of the $C_4O_4^{2-}$ ligand (Scheme 1p for **1** and Scheme 1o for **2**).

3.2 TGA and X-ray Powder Diffraction (XRPD)

The experimental and computer-simulated XRPDs confirm the purity of **1** and **2** (Fig. S2). The thermal stability of **1** and **2** were performed on single-phase polycrystalline samples from 20 to 800 °C. The TGA curve (Fig. S3) shows that **1** is thermally stable up to 370 °C, and thereafter significant weight loss occurs resulting in complete decomposition of the compound. The final residual weight is likely attributed to ZnO (calc. 58.8 % and exp. 58.1 %). While for **2**, the TGA demonstrates that **2** shows a two-step weight loss and the sample is thermally stable up to170 °C. The first weight loss is 6.7 % from 170 to 210 °C and corresponds to the loss of coordination water molecules (calcd. 7.8 %). And the anhydrous composition is stable up to 320 °C. After 320 °C, the framework of **2** rapid collapses until 480 °C, which is attributed to the decomposition of **2**. The total mass loss of 43.9 % corresponds to the removal of the organic species (calc. 44.3 %). The remaining weight (56.1 %) corresponds to CdO.

3.3 Fluorescent Property

Taking into account the excellent luminescent properties of d^{10} metal complexes, the solid-state luminescence of compounds **1** and **2** at room temperature was investigated

(Fig. 6). It can be observed that the fluorescence emission occurs at around 396 nm for **1**, under $\lambda_{ex} = 247$ nm, whereas no detectable emission occurs for **2** under $\lambda_{ex} = 247$ nm. To understand the nature of the emission band, the photoluminescence property of the squaric acid ligand was also analyzed. It found that two emission bands at 284 and 396 nm could be observed for free squaric acid ligand under $\lambda_{ex} = 240$ nm. For **1**, the complete quenching of the emission peak at 286 nm is probably attributed to the hydroxyl O–H oscillators [29]. And compound **2** does not exhibit detectable emission probably due to the quenching effects of the aqua ligands [30, 31].

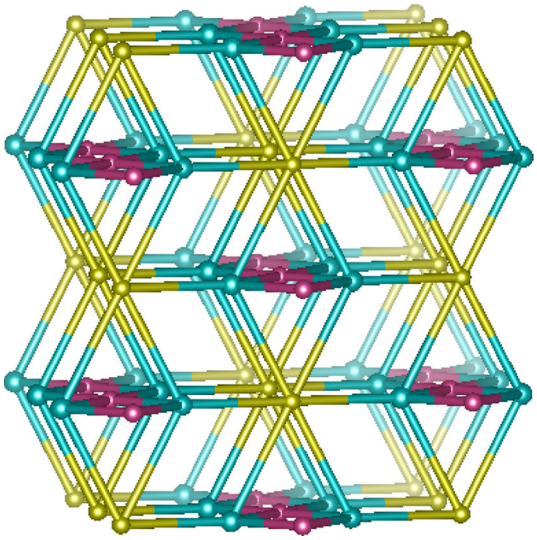

Fig. 5 Schematic representation of the trinodal (4,5,6)-connected network of **2**. Color codes: *blue* for 5-connected Cd(II), *golden* for 6-connected $C_4O_4^{2-}$ ligand and *purple* for 4-connected OX^{2-} ligand (Color figure online)

4 Conclusions

In summary, two new 3D polymeric Zn(II)/Cd(II)-networks have been successfully isolated under hydrothermal condition by reaction of squaric acid and different d^{10} metal salts. The different topological nets of compounds **1** and **2** are mainly caused by the different coordination modes of squarate. In addition, compared to squaric acid ligand, compound **1** and **2** have obvious fluorescence quenching due to the O–H vibrational excitation from the *u*-OH and the aqua ligand. Further investigations for the influence of d^{10} metal ions on squarate-based coordination frameworks are ongoing in our lab.

5 Supplementary Materials

CCDC 1010496 and 1010497 for **1** and **2**, respectively, contain the supplementary crystallographic data for this paper. These CIF data can also be obtained free of charge from the Cambridge Crystallographic Data Centre via http://www.ccdc.cam.ac.uk/data_request/cif, or from the Cambridge Crystallographic Data Centre, 12 Union Road, Cambridges CB2 1EZ, UK; fax: (+ 44) 1223-336-033; or

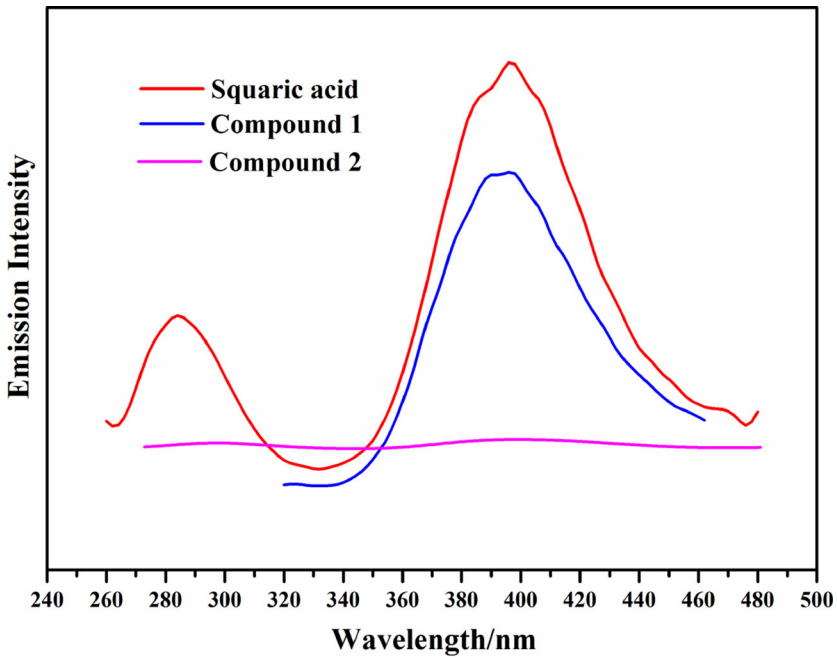

Fig. 6 Solid-state emission spectra of squaric acid, **1** and **2** at room temperature (Color figure online)

email: deposit@ccdc.cam.ac.uk. Addition structural figures, TG and powder X-ray patterns can be found in the supporting file. Supplementary data associated with this article can be found, in the online version.

Acknowledgments This work was financially supported by the NSF of China (Nos.: 21301106 and 21201109), the NSF of Hubei Province of China (2011CDA118), the Project of Hubei Provincial Education Office (Q20131304).

References

1. Y. Yue, Z.A. Qiao, P.F. Fulvio, A.J. Binder, C. Tian, J. Chen, S. Dai, J. Am. Chem. Soc. **135**, 9572 (2013)
2. D.N. Bowman, J.H. Blew, T. Tsuchiya, E. Jakubikova, Inorg. Chem. **52**, 8621 (2013)
3. D.S. Li, Y.P. Wu, J. Zhao, J. Zhang, J.Y. Lu, Coord. Chem. Rev. **261**, 1 (2014)
4. T. Li, F.L. Wang, S.T. Wu, X.H. Huang, S.M. Chen, C.C. Huang, Cryst. Growth Des. **8**, 3271 (2013)
5. D.S. Li, J. Zhao, Y.P. Wu, B. Liu, L. Bai, K. Zou, M. Du, Inorg. Chem. **52**, 8091 (2013)
6. W.W. Dong, D.S. Li, J. Zhao, L.F. Ma, Y.P. Wu, Y.P. Duan, CrystEngComm. **15**, 5412 (2013)
7. S. Chen, R.Q. Fan, C.F. Sun, P. Wang, Y.L. Yang, Q. Su, Y. Mu, Cryst. Growth Des. **12**, 1337 (2012)
8. Y.P. He, Y.X. Tan, J. Zhang, Inorg. Chem. **52**, 12758 (2013)
9. T. Li, M.T. Kozlowski, E.A. Doud, M.N. Blakely, N.L. Rosi, J. Am. Chem. Soc. **135**, 11688 (2013)
10. T. Li, X. Liu, Z.P. Huang, Q. Lin, C.L. Lin, Q.G. Zhan, X.D. Xu, Y.P. Cai, Inorg. Chem. Commun. **39**, 70 (2014)
11. C.C. Wang, C.H. Yang, G.H. Lee, Eur. J. Inorg. Chem. **2006**, 820 (2006)
12. C.C. Wang, W.C. Chung, H.W. Lin, S.C. Dai, J.S. Shiu, G.H. Lee, H.S. Sheu, W. Lee, CrystEngComm. **13**, 2130 (2011)
13. H. Erer, O.Z. Yesilel, N. Dege, Y.B. Alpaslan, J. Inorg. Organomet. Polym. Mater. **20**, 411 (2010)
14. H.Y. Zang, H.N. Miras, J. Yan, D.L. Long, L. Cronin, J. Am. Chem. Soc. **124**, 11376 (2012)
15. C.C. Wang, C.T. Kuo, J.C. Yang, G.H. Lee, W.J. Shih, H.S. Sheu, Cryst. Growth Des. **7**, 1476 (2007)
16. P. Millett, L. Sabadie, J. Galy, J.C. Trombe, J. Solid State Chem. **173**, 49 (2003)
17. A. Bouayad, J.C. Trombe, A. Gleizes, Inorg. Chim. Acta **230**, 1 (1995)
18. S.L. Georgopoulos, R. Diniz, B.L. Rodrigues, L.F.C.D. Oliveira, J. Mol. Struct. **741**, 61 (2005)
19. R.A. Mole, J.A. Stride, P.F. Henry, M. Hoelzel, A. Senyshyn, A. Alberola, C.J.G. Garcia, P.R. Raithby, P.T. Wood, Inorg. Chem. **50**, 2246 (2011)
20. R.A. Mole, M.A. Nadeem, J.A. Stride, V.K. Peterson, P.T. Wood, Inorg. Chem. **52**, 13462 (2013)
21. X.J. Ke, D.S. Li, J. Zhao, L. Bai, J.J Yang, Y.P. Duan. Inorg. Chem. Commun. **21**, 129 (2012)
22. Rigaku, CrystalClear. Rigaku Americas, The Woodlands, Texas, USA, and Rigaku Corporation, Tokyo, Japan (2011)
23. G.M. Sheldrick, Acta Crystallogr. **A64**, 112 (2008)
24. X.H. Be, M.L. Rong, H.C. Chang, S. Kitagawa, S.R. Batten, Angew. Chem. Int. Ed. **43**, 192 (2004)
25. L. Cunha-Silva, R. Ahmad, M.J. Carr, A. Franken, J.D. Kennedy, M.J. Hardie, Cryst. Growth Des. **7**, 658 (2007)
26. A.A. Khandar, J. White, T. Taghvaee-Yazdeli, S.A. Hosseini-Yazdi, P. Mcardle, Inorg. Chim. Acta **400**, 203 (2013)
27. X.Z. Wang, D.R. Zhu, Y. Xu, J. Yang, X. Shen, J. Zhou, N. Fei, X.K. Ke, L.M. Peng, Cryst. Growth Des. **10**, 887 (2010)
28. A. Jabłońska-Wawrzycka, K. Stadnicka, J. Masternak, M. Zienkiewicz, J. Mol. Struct. **1012**, 97 (2012)
29. H.B. Xu, J. Li, L.Y. Zhang, X. Huang, B. Li, Z.N. Chen, Cryst. Growth Des. **10**, 4101 (2010)
30. Y.L. Gai, F.L. Jiang, K.C. Xiong, L. Chen, D.Q. Yuan, L.J. Zhang, K. Zhou, M.C. Hong, Cryst. Growth Des. **12**, 2079 (2012)
31. M.D. Allendorf, C.A. Bauer, R.K. Bhakta, R.J. Houk, Chem. Soc. Rev. **38**, 1330 (2009)